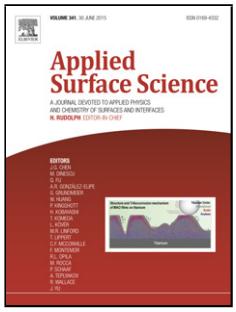

Title: Structural, Morphological, Compositional and Optical Studies of Plasma Polymerized 2-Furaldehyde Amorphous Thin Films

Authors: Humayun Kabir, M. Mahbubur Rahman, Kabir M. Uddin, A.H. Bhuiyan

PII: S0169-4332(17)31939-6
DOI: http://dx.doi.org/doi:10.1016/j.apsusc.2017.06.284
Reference: APSUSC 36484

To appear in: *APSUSC*

Received date: 21-3-2017
Revised date: 22-6-2017
Accepted date: 27-6-2017

Please cite this article as: Humayun Kabir, M.Mahbubur Rahman, Kabir M.Uddin, A.H.Bhuiyan, Structural, Morphological, Compositional and Optical Studies of Plasma Polymerized 2-Furaldehyde Amorphous Thin Films, Applied Surface Sciencehttp://dx.doi.org/10.1016/j.apsusc.2017.06.284

Structural, Morphological, Compositional and Optical Studies of Plasma Polymerized 2-Furaldehyde Amorphous Thin Films

HumayunKabir[a,b*], M. MahbuburRahman[a,c],Kabir M. Uddin[c], A. H. Bhuiyan[d]

[a]Department of Physics, Jahangirnagar University, Savar, Dhaka 1342, Bangladesh

[b]School of Metallurgy and Materials, University of Birmingham, Edgbaston, Birmingham B15 2TT, United Kingdom

[c]Surface Analysis and Materials Engineering Research Group
School of Engineering & Information Technology, Murdoch University, Perth, Western Australia 6150, Australia

[d]Department of Physics, Bangladesh University of Engineering and Technology, Dhaka 1000, Bangladesh

Corresponding Author's email: hxk598@bham.ac.uk

Graphical abstract

Thickness, $t \pm 5$ (nm)	Direct band gap, E_{dg} (eV) ± 0.01	Indirect band gap, E_{ig} (eV) ±0.01	Band edge sharpness, P_s ($cm^{-2}eV^{-1}$) ±0.02	Urbach energy, E_u (eV) ± 0.01	Steepness parameter, σ ± 0.001
100	3.40	2.20	3.32×10^{-8}	0.59	0.044
180	3.41	2.15	1.58×10^{-8}	0.61	0.042
250	3.42	2.10	2.20×10^{-8}	0.56	0.046
300	3.45	2.45	4.50×10^{-8}	0.50	0.051

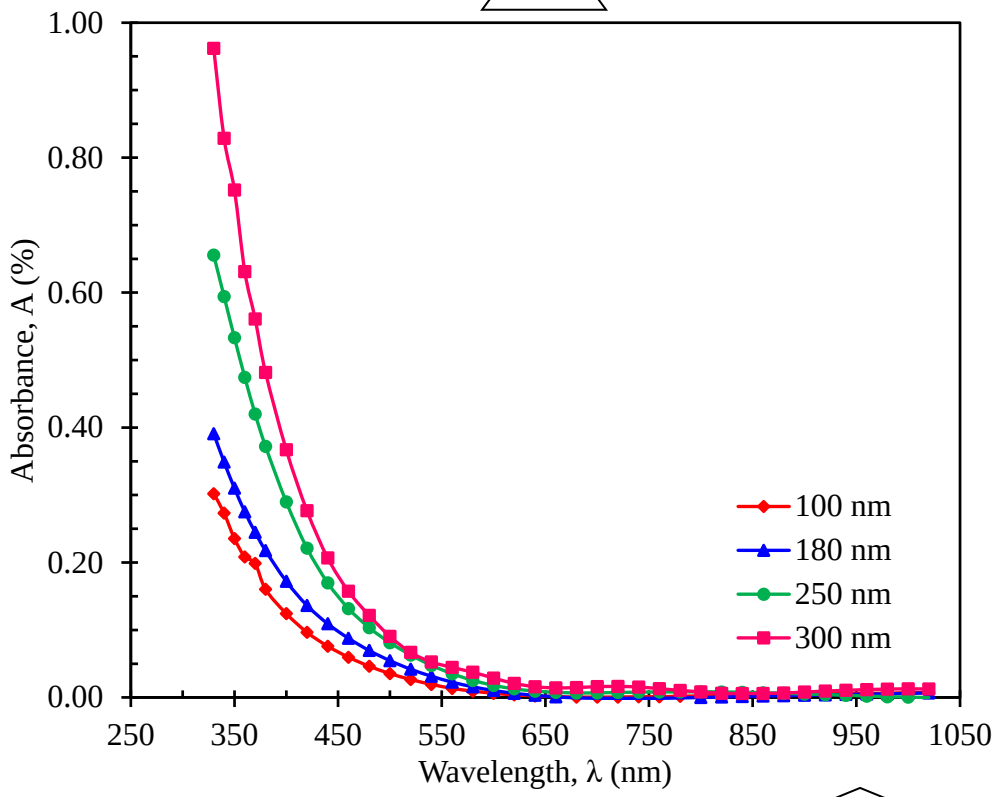

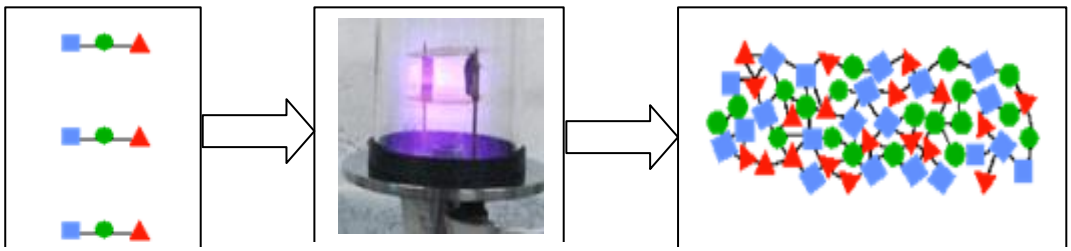

Monomer Plasma Polymerization Plasma Polymer

Highlights

- Plasma polymerized 2-furaldehyde thin films of different thicknesses were deposited onto glass substrate in optimum conditions by glow discharge reactor.
- XRD results confirmed the amorphous nature of the films.
- The as-deposited PPFDH thin films contain asymmetric C-H and C≡C stretching bonds due to plasma polymerization.
- The direct and indirect optical band gaps of the PPFDH thin films of different thicknesses were found to be 3.40-3.45 and 2.10- 2.45 eV, respectively.
- The dispersion energy increases from 6.35 to 18.85 eV while oscillator energy decreases from 3.17 to 2.83 eV with increasing thickness of the thin films.

Abstract

Plasma synthesized 2-furaldehyde (PPFDH) amorphous polymer thin films of varying thicknesses were prepared in optimum conditions by a capacitively coupled parallel plate glow discharge reactor at room temperature. The structure, morphology, composition and optical properties of deposited PPFDH thin films have been investigated using X-Ray diffraction (XRD), Fourier transform infrared (FTIR) spectroscopy, Scanning electron microscopy (SEM), Energy dispersive X-Ray spectroscopy (EDS), as well asUltraviolet–visible (UV-Vis) absorption spectroscopy. XRD results confirmed the amorphous nature of the films. The smooth and uniform nature of the PPFDH thin films were observed by SEM images. FTIR analyses of monomer FDH and PPFDH thin films show that structural rearrangement has occurred due to the synthesis process taking place in the chemical structure. IR stretching bands obtained from DFT calculations of the optimized structuresof monomer and polymer of2-furaldehyde are in good agreement with the experimental results. UV-Vis absorption spectra in transmittance as well as reflectance mode were utilized to compute absorption coefficient, allowed direct and indirect transition energy gaps, band edge sharpness, Urbach energy, steepness parameter, extinction coefficient, and dispersion and oscillator energy. The oscillator strength, moments of optical spectra, refractive index at infinite wavelength, high frequency dielectric constant, average oscilator strength, complex refractive index, dissipation factor, optical conductivity and skin depth were also determined by using measured UV-Vis transmittance and reflectance spectra.

Keywords: 2-furaldehyde, glow discharge reactor, UV-Vis absorption spectroscopy, transition energy gaps, Urbach energy and dissipation factor.

1. Introduction

Over the last several decades, the interest in organic thin films has been increasing because of their striking properties. Their relevance has been ina number of areas such as mechanics, electronics and optics comprising chemical, physical and biological sensors, coatings for chemical fibers and films, microelectronic devices, passivation of metals, nonlinear optical device, sacrificial layers, molecular devices, surface hardening of tool, spaceship components, etc. [1-3]. Thin films of organic compounds havepotential inflictions in various electronic devices including organic solar cells, LEDs, photo detectors, lasers and thin film transitions [4-5]. The films which are prepared by plasma polymerization (PP) usually have improved quality and are uniform, adherent, thermally durable and free of pinholes [6-8]. Polymer filmssynthesized by the PP techniqueare used as dielectric, optical devices and optical coatings to inhibit corrosion. Therefore, the study of their optical properties is of particular interest [9]. The plasma assisted method is the fastest developing area of research in thin film preparation from new polymeric materials that are almost impossible to prepare via conventional polymerization techniques. The usage of glow discharges to polymerize a variety of organic and organometallic compounds has been on the increase [10]. The PP technique has unique practical benefits including confirmative ultra-thin film preparation, excellent adhesion with substrate and chemically and physically viable surfaces [11]. This technique can be used to adhere thin films onto nearly all substrates. Moreover, it is not necessary to use solvent and complex geometries as adhesion can be achieved in one step. Moreover, using this method it is possible to prepare thin films of organic materialsfrom any volatile organic or organometallic molecule [12-17]. Commonly, a polymer synthesized by the PP method does not contain the structure of the onset monomers; consequently, to subsume the clearly-defined chemical functionalities of a precursor molecule, the deposition is normally performed under light states to decrease fragmentation modes. The significant techniques to acquire that kind of functional polymer films includethermal evaporation [18, 19], solution cast [20], electro-deposition [21], plasma polymerization [22-24], sol-gel [25, 26], atomic layer deposition [27], RF magnetron sputtering [28-29], ion beam sputtering [30], plasma enhanced chemical vapor deposition [31], chemical vapour deposition (CVD) [32], and pulsed plasma CVD [33], etc. The PP technique is highly recommended since it is

capable of fabricating very thin films that could not be prepared by using other techniques and almost all organic vapors can be used to form polymer thin films. For industrial use, polymer thin films obtained via this technique produces coating with excellent adhesion on nearly entire substrates, superb mechanical, thermal, and chemical durability, cross-linked, and pinhole-free natures, etc. Many researchers have studied PP thin polymer films in order to understand the structural, morphological, optical, thermal and electrical behavior and to find their potential applications [34-41]. Matin and Bhuiyan synthesized PP 2,6 diethylaniline (PPDEA) thin films and structural rearrangement was observed during the synthesis process. The reported direct and indirect band gaps of the PPDEA films were about 3.60 and 2.23 to 2.38 eV respectively for different thicknesses. The Urbach energy decreased from0.65 to 0.47eV while the steepness parameter increased from 0.030 to 0.055 with increasing thickness [42]. Blaszczyk-Lezak *et al*. [43] studied the preparation and optical analysis of PP perylene films at varying thicknesses and observed that films are highly absorbent and fluorescent having RMS roughness within 0.3-0.4 nm. Cho *et al.* [44] reported physical and electrical behaviours of PP as-grown and the annealed pure ethylcyclohexane thin films at several deposition RF powers and annealing temperatures via plasma enhanced chemical vapor deposition (PECVD). The FTIR spectra showed that the PP thin films had entirely different chemical structures from those of the monomer ethylcyclohexane. They also observed shrinkage (%) in the thicknesses of the thin films before and after the annealing. Afroze and Bhuiyan [45] investigated the PP 1, 1, 3, 3-tetramethoxy-propane films and observed smooth, uniform and pinhole free films with C=C and C=O bonds. Optical properties of PP pyrrole-N, N, 3, 5-tetramethylaniline (PPTMA) bilayer films were studied by Kamal and Bhuiyan [46]. Allowed direct (E_{qd}) and allowed indirect (E_{qi}) energy gaps were estimated using UV-Visible absorption spectra and the obtained value ofE_{qd} for PPPy, PPPTMA and PPPy-PPTMA bilayer films were 3.30, 2.85 and 3.65 eV while E_{qi} were 2.25, 1.80 and 2.35 eV, respectively. Sarker and Bhuiyan prepared and investigated PP 1-benzyl-2-methylimidazole (PPBMI) films. SEM analysis confirmed its uniform and flawless nature while FTIR analysis illustrated the functional group present in PPBMI films. The obtained value of E_{qd} and E_{qi} of prepared PPBMI were found to be in the range of 3.10-3.35 eV and 1.80-1.95 eV respectively. They also found that both E_{qd} and E_{qi} increase with increasing thickness and decrease upon annealing [47]. Majumder and Bhuiyan [48] employed electrical glow discharge to prepare PP vinylene carbonate (PPVC) thin films samples and reported that surface of the PPVC are smooth as well as pinhole free. The increased nature of absorbance was also cited with the increasing film thickness. The variation of the optical characteristics

of PPDEA films by iodine doping was investigated by Matin and Bhuiyan [49] and they reported a substantial reduction of the energy band-gap due to iodine doping. The value of E_{qd} was decreased from 3.56 to 2.79 eV while that of E_{qi} was reduced from 2.23 to 1.97 eV with the increase of doping period. Keeping these facts in mind, the 2-furaldehyde (FDH) was taken as monomer in this study. This is because FDH is a derivate of furan and is anticipated that it will offer thin films having fascinating properties in a plasma glow discharge. Although citations on the synthesis and structural, morphological, compositional as well asoptical characterizations of ac PPFDH thin films are carried out but the amount of studies are very limited and require more insightful analysis. As such this paper seeks a better understandingon the estimation of band-energy sharpness, Urbach-energy and steepness parameter of plasma polymerized PPFDH films using the UV-visible absorbance spectral distribution. In addition to these, structural, morphological and elemental analysis of the plasma polymerized PPFDH films are also reported. The electrical conduction mechanism of these films has been cited in our more recent study [50].

2. Experimental details

2.1. Sample preparation

2.1.1. Themonomer

The monomer, 2-furaldehyde (FDH) in liquid formwas used as aprecursor in this research work andmanufactured by BDH Chemicals Ltd., Poole, England. The chemical structure of FDH is illustrated in Fig.1and its typical properties are stated in Table 1.

2.1.2. Preparation of plasma polymer thin films

The monomer FDH was deposited onto glass substrates having dimension of $(2.54\times7.62\times0.12)\times10^{-2}$ m (Sail Brand, China) to produce PPFDH films using a cylindrical shape capacitively paired glow discharge system. The system contains two circular plate electrodes made by stainless steel having a diameter 9×10^{-2} m and thickness 1×10^{-3} m, positioned at a distance about 4×10^{-2} m. Plasma was produced on all sides of the glass substrates which were put on the lower electrode, utilizing a step up transformer connected to the electrodes with a power of about 40 W at line frequency, 50 Hz. A rotary pump (Vacuubrand GMBH &Co., Germany) was used to maintain the pressure of the chamber at about 1.33 Pa. The FDH vapor was injected into the chamber by a flow meter at an approximate constant rate of 20 cm^3 min^{-1}. The deposition duration was altered in between 30

to 90 minutes to obtain PPFDH with different thicknesses. The thickness, *t* of theprepared PPFDH films was measured via the Multiple-Beam Interferometry method using equation [51],

$$t = \frac{\lambda y}{2x} \quad (1)$$

Where λ (= 589.3 nm) is the wavelength of the used monochromatic Na light used as a source, *y* the step height and *x* the width of the Fizeau fringes. The values of *y* and *x* were measured by a traveling microscope. The fringe patterns obtained from PPFDH films are portrayed in Fig. 2.

2.2. Characterization technique

2.2.1. X-ray diffraction (XRD) analysis

X-ray diffraction patterns of PPFDH thin films were obtained using a Equinox 3000 (Inel France Z.A. - C.D. 405 45410 Artenay, France) Powder X-ray diffractometer using Cu-K_α radiation of wavelength 1.5406 Å, operated at a voltage of 40 kV and current 40 mA, with high temperature attachment up to 1600 ^{0}C. The XRD scan was recorded in 2θ scans with a grazing incidence angle of 1°, an angular interval (10° to 90°), a step size 0.03°, and acount time 2 s per step.

2.2.2. Fourier transform infrared (FTIR) spectroscopy

To study the chemical structure of the FDH and PPFDH, the FTIR spectra were recorded. The powder of the PPFDH was taken out from the PPFDH deposited onto glass substrates. A drop of liquid monomer was put in a KBr measuring cell to find the spectra of FDH while for recording FTIR spectra of PPFDH; pellets of KBr with 2% PPFDH powder were made. A dual beam FTIR spectrophotometer (SHIMADZU FTIR-8900 spectrophotometer, Japan) was used to record FTIR spectra of FDH as well as PPFDH at room temperature. The spectra were recorded in transmittance (%) mode in the wavenumber range 400-4000 cm^{-1}.

2.2.3. Scanning electron microscopy (SEM) and electron dispersive X-ray (EDS) analysis

Small pieces of chemically cleaned glass substrates were used to deposit PPFDH thin films for SEM and EDS analyses. A thin layer of gold was deposited on the PPFDH films via sputtering (AGAR Auto Sputter Coater) to eliminate the charging effect. A scanning electron microscope (Model: S-3400 N, Hitachi, Japan) was used to take SEM micrographs and EDSspectra of PPFDH films. The operating voltage, spot size and spatial resolution of SEM were 20 kV, 3 and 5 nm, respectively.

2.2.4. Ultraviolet–visible (UV-Vis) absorption spectroscopy

In the case of UV-Vis spectroscopic measurements, the PPFDH films were coated on the glass substrate havinga dimension of (18×18×2) mm (Marienfeld, Germany).The UV-Vis spectra of as-deposited PPFDH films were recordedby a Shimadzu UV-160A spectrophotometer (Shimadzu, Japan) at room temperature intransmittance as well as reflectance mode in the wavelength range 250-1050 nm. A blank glass slide was used in this experiment as reference.

2.3. Computational method

All calculations were performed using Gaussian09 [52]. The geometries of 2-furaldehyde was fully optimized with density functional theory (DFT) using B3LYP/6-31G (d,p) level of theory. Vibrational frequencies obtained for structural parameters of the monomer (Fig. 3a) and a few polymers (Fig. 3a□3b) of 2-furaldehyde presented in Table 2 were obtained using B3LYP/6-31G (d,p).

3. Results and discussion

3.1. Structural analysis of PPFDH

3.1.1. XRD analysis

In order to investigate the crystalline nature of PPFDH thin films, XRD measurements were taken. The XRD profiles of the as-deposited PPFDH thin films of thicknesses 100, 180, 250 and 300 nm are presented in Fig.4. It is observed that there is no remarkable peak in the XRD patterns. It is therefore concluded that all these films are entirely amorphous in nature [53].

3.1.2. FTIR analysis

The FTIR spectra of the monomer FDH and as-deposited PPFDH at different thicknesses are illustrated by A, B, C, D and E respectively in Fig. 5. The structure changes caused by the plasma polymerized synthesis process are confirmed by these FTIR spectra. In spectrum A, at a wavenumber about 3154 cm^{-1}, a broad band is found which shows the presence of O-H stretching vibration which is due to absorbed water. The wider bands observed at 2872 cm^{-1} and 2823 cm^{-1} might be due to aliphatic -O-CH_3 attached to FDH. The non-conjugated C=O stretching vibration band at 1709 cm^{-1} is observed in FDH. The absorption bands at 1495 and 1423 cm^{-1} are due to asymmetric C-H bending. The band at 1318 cm^{-1} represents the symmetric C-H bending vibration of -CH_3. The absorption band at 1177 cm^{-1} is for C-C skeletal vibration. The band at 1054 cm^{-1} in spectrum A indicates C-H in plane bending. The absorption band at 961 cm^{-1} is due to C-H rocking. The sharp peaks at 754 cm^{-1} may have appeared because of =C-H out-of-plane bending, and the C=C out of plane bendingis obtained at 607 cm^{-1}. A good agreement between the experimental results and theoretical predictions (see Table 2 and Fig. 6), were observed for monomer FDH.

In spectrum B, C, D and E of the as deposited PPFDH thin films at different thicknesses, the absorption band at 3407 cm^{-1} (B), 3380 cm^{-1} (C), 3379 cm^{-1} (D) and 3377 cm^{-1} (E) may be observed as a results of O-H stretching vibrations, which is like in (A). The bands which resulted at 2926 (B), 2949 (C), 2948 (D) and 2954 cm^{-1} (E) may be due to C-H stretching. The C≡C in B, C and D at 2202, 2221and 2221 cm^{-1} may arise due to plasma polymerization. The sharp absorption peaks at 1603 (B), 1671 (C), 1670 (D) and 1633 (E) cm^{-1} may have occurreddue to C=C stretching vibration and conjugation during polymerization. The bands at around 1261, 1261 and 1268 cm^{-1} in C, D and E respectively is owing to C-H twisting and band at 1161 cm^{-1} in B indicates a C-C skeletal vibration. Strong bands at 586, 672, 671 and 655& 532 cm^{-1} in B, C, D and E respectively show the C=C out of plane bending. The location of all the band frequencies and their corresponding modes of vibration are recorded in Table 2 for comparison. However, the IR stretching bands of the polymer (Fig. 3b) structures of 2-furaldehyde is also in good agreement with theoretical values (Table 2) as shown in Fig. 7.

3.2. Morphological and elemental analysis of PPFDH

3.2.1. SEM analysis

SEM images of PPFDH films of different thicknesses were performed at 20 kV and with different magnifications of 25k× and 50k×, as illustrated in Fig. 8 and Fig. 9, respectively. From SEM analysis, it can be concluded that all of the PPFDH thin films surfaces are uniform and fracture free. It is also observed that there is no pin hole present in the as deposited films. Similar results have previously been reported [54].

3.2.2. EDS analysis

The EDS connected to the SEM was used to study the compositionof the PPFDH films. The weight percentage (wt. %) of the different elements present in the monomer FDH as well as prepared PPFDH films are listed in Table 3. The results confirmed the existence of Carbon (C), Oxygen (O) and unwanted Sodium (Na), Magnesium (Mg), Silicon (Si) and Calcium (Ca) in all types of PPFDH thin films. From the results it was observed that C has the maximal % and the presence of O follows an excellent ratio as we can predict from the monomer FDH. The excessive% of O in the PPFDH thin films is due to the incorporation of ambient O when samples were received from the reactor chamber. The availability of Na, Mg, Si and Ca as presented in EDS analyses of the PPFDH sample was absent in the FDH sample might be appeared because of the substrate material. Conversely, EDS cannot identify the hydrogen present in the PPFDH thin films.

3.3. Optical analysis of PPFDH

3.3.1. Spectral distribution of the transmittance and reflectance

The optical properties of the PPFDH thin films at various thicknesses were investigated by means of UV-Vis spectroscopy analysis in the wavelength region 250-1050 nm. The study of the optical absorption of the studied thin films, especially the absorption edge has proved very effective for determination of the electronic structure of thematerials. In this case, transmittance $T(\lambda)$ and reflectance $R(\lambda)$ spectra were studied for PPFDH thin films at 100 nm, 180 nm, 250 nm and 300 nm thicknesses in the wavelength range of 250-1050 nm at room temperature.The variation of $T(\lambda)$ and $R(\lambda)$ with wavelength, λarepictured in Fig. 10 and Fig. 11, respectively. It is clear from Fig. 10 that, the optical transmittance increases with increasing wavelength but decreases with thickness of the PPFDH thin films and becomes almost constant at higher wavelength while reverse nature is observed for reflectance spectra.

3.3.2. Optical band gaps and band edge sharpness determination

The absorption coefficient, α can be calculated using the experimentally measured transmittance data for various λ corresponding to varied photon energies, $h\nu$ at room temperature by the equation given below [55]:

$$\alpha = \frac{1}{t}\ln[\frac{(1-R^2)}{T}] \qquad (2)$$

where t is the thickness of the thin film. The change of α with λ for entire PPFDH samples is portrayed in Fig. 12. It has been observed from Fig. 12 that the values of α monotonically decrease with increase of λ for all the as-deposited samples while absorption is found to be absent in the visible region which predicts the insulating nature of the films [56]. It also be noticed that the curves possess two distinct gradients in the experimental photon energy range. This may indicate the existence of direct and indirect optical transitions in the prepared films. These exponential falling edges may either be due to lack of long-range order or due to the existence of defects in the films. In case of materials which have crystalline and amorphous nature, photon absorption is found to be obey the Tauc equation [57],

$$\alpha h\nu = P\,(h\nu - E_q)^n \qquad (3)$$

Where, P is a constant not connected to the energy, E_g the optical energy band gap and n is parameter that characterizes the nature of band transition. The value of n =1/2 and 2 correspond to direct and indirect allowed transitions, respectively while that of 3/2 and 3 indicate direct and indirect forbidden transitions, respectively. The E_q can be estimated from extrapolation of the straight-line part of the $(\alpha h\nu)^{1/n}$ against $h\nu$ graph to $h\nu$ = 0. The values of direct band gap, E_{dq} and indirect band gap, E_{iq} were computed from the plots $(\alpha h\nu)^2$ against $h\nu$ and $(\alpha h\nu)^{1/2}$against $h\nu$, respectively which are shown in Figs. 13–14. The band edge sharpness value, P_s was obtained from the gradient of the $(\alpha h\nu)^2$ against $h\nu$ graph in the range of band-to-band absorption [58]. The values of E_{dq}, E_{iq} and P_s for all PPFDH films are noted in Table 4. It is observed that the value E_{dq} is almost constant where as the value of E_{iq} decreases with increasing thickness except the sample having thickness 300 nm. This might be owing to the possible structural defects in the samples that incorporated during their synthesis [59].

3.3.3. Urbach energy and steepness parameters of PPFDH films

Generally, the spectral reliance of α is investigated in the region of the photon energies under the energy gapof the films. That is in a region called Urbach spectral tail that

indicates the gradient of the exponential edge. In the region of the Urbach spectral tail, the relation between α and photon energy, E can be revealed as [60],

$$\alpha = \alpha_0 exp(E / E_u) \quad (4)$$

where α_0 is a constant and E_u the Urbach energy. The E_u can be worked out as the breadth of the exponential absorption border or as the breadth of the tails of localized states. The graph obtained by plotting lnα against hv should be linear whose gradient provides value of E_u. The lnα vs hv plots for all as deposited PPFDH thin films are represented in Fig.15 and the estimated values of $E_u$are recorded in Table 4. It is observed that the values of E_u, the band width of the localized states, decreases as the thickness increases, except the film having thickness of 180 nm. This behaviour of the Urbach energy with thickness of the films was observed by Matin and Bhuiyan [42] and this nature may be obtained because of the reduction of the degree of disorder as well as the density of defect states [42, 61]. The steepness parameter, σ which represents the broadening of the optical absorption end because of the electron phonon or exciton-phonon interactions [62], could be computed with the following relation,

$$\sigma = kT / E_u \quad (5)$$

where k is the Boltzmann constant and T the absolute temperature. In calculation of σ in this study, the value of T was 298K. The calculated values of σ are noted in Table 4. The value of α as well as λ can be used to find the values of extinction coefficient, K by using the simple equation,

$$\alpha = 4\pi K / \lambda \quad (6)$$

The variation of K for PPFDH thin films with hv is shown in Fig.16. The plot indicates the increasing nature of K with the increase in hv. This might be due to the probabilities of electron transfer across the mobilitygap.

3.3.4. Dispersion energy parametersof PPFDH films

The refractive index dispersion plays a vital role in the research for materials containing enhance optical properties, owing to the fact that it is a significant factor in optical communication and in designing devices where spectral dispersion is guiding factor. Therefore, it is significant to work out dispersion parameters of the films [63]. Wemple and Didomenico [64] use a single-oscillator model to describe frequencydependent dielectric constant to find dispersion energy parameters. The dispersion parameters of the films were evaluated using the following relation [65, 66],

$$(n^2-1)^{-1} = \frac{E_0^2 - (h\nu)^2}{E_0 E_d} \quad (7)$$

where n, $h\nu$, E_0 and E_d is the refractive index, photon energy, oscillator energy and dispersion energy, respectively. The oscillator energy, E_0 indicates the mean energy gap usually defined as the energy separation between the centers of both the conduction and the valence bands whereas dispersion energy, E_d is a measure of the mean strength of the inter band optical transitions and represents the natural electronic excitation spectrum. For semiconductors and insulators, where the K and n are related as $K^2 << n^2$, the relationship between R and n is given by [67, 68],

$$R = \frac{(n-1)^2 + K^2}{(n+1)^2 + K^2} \quad (8)$$

For insulating materials equation (7) can be simplified and rearranged as follows,

$$n = \frac{1+\sqrt{R}}{1-\sqrt{R}} \quad (9)$$

The computed value of n with varied wavelength, λ is presented in Fig. 17. The value of n monotonically rises with the increment of the value of λ. The values of E_d and E_o can be evaluated from the plot of $(n^2\text{-}1)^{-1}$ versus $(h\nu)^2$ as shown in Fig. 18. By taking the intercept of the extrapolation of the curve in Fig. 18, the value of E_d was computed while the value of E_o was found from the gradientof the curve of Fig. 18. The gradient of the curve and intercept on the vertical axis give $(E_dE_o)^{-1}$and (E_0/E_d), respectively. The oscillator strength, f were calculated by multiplying the values of E_d and E_o. The moments of optical spectra M_{-1} and M_{-3} was determined by the following equations [60, 69].

$$E_0^2 = \frac{M_{-1}}{M_{-3}} \quad (10)$$

$$E_d^2 = \frac{M_{-1}^3}{M_{-3}} \quad (11)$$

The obtained values of E_o, E_d, M_{-1}, M_{-3} and f are tabulated in Table 5. It is observed that with increase of thickness the values of E_d, M_{-1}, M_{-3} and f increased but the values of E_o decreased. The refractive index at infinite wavelength (λ_∞), n_∞ and high frequency dielectric constant, ε_∞ were evaluated by the straight forward classical dispersion equation [69, 70],

$$\frac{n_\infty^2 - 1}{n^2 - 1} = 1 - (\frac{\lambda_\infty}{\lambda})^2 \quad (12)$$

The $(n^2\text{-}1)^{-1}$ versus λ^{-2} was plotted in Fig. 19 to determine the values of n_∞ for PPFDH thin films. The intersection with $(n^2\text{-}1)^{-1}$ gives $(n_\infty^2 - 1)^{-1}$ and hence n_∞^2 at λ_∞ equal to ε_∞. The

obtained values of n_∞ and ε_∞ for PPFDH files are noted in Table 6. Eq. (11) can be re-written as [71]:

$$n^2 - 1 = \left(\frac{S_0 \lambda_\infty}{1 - \left(\frac{\lambda^2}{\lambda_\infty^2} \right)} \right) \qquad (13)$$

Where $\frac{(n_\infty^2 - 1)}{\lambda_\infty^2} = S_0$ is the average oscilator strength. The values of S_0 and λ_∞ were computed experimentally by the plot of $(n^2\text{-}1)^{-1}$versusλ^{-2} as presented in Fig. 19. The tangent of the straightline portion provides $1/S_o$ and intercept at the infinite λ presents$\frac{1}{S_0 \lambda_\infty^2}$. The obtained values of S_0 and λ_∞ are noted in Table 6. It is observed that obtained values changes with thickness of the synthesized thin films. Similar result were reported some other researchers [72, 73].

3.3.5. Complex dielectric constant and Optical conductivity of PPFDH films

The complex refractive index $\hat{n} = n + ik$ and dielectric function $\hat{\varepsilon} = \varepsilon_r + i\varepsilon_i$ indicate the optical characteristics of any solid materials. Therefore, it is important to investigate complex dielectric constant to find information about electronic structure of the deposited thin films. The real and imaginary parts of dielectric constant (ε_r and ε_i) of thin films can be evaluated by two subsequent equations [74, 75]:

$$\varepsilon_r = n^2 - K^2 \qquad (14)$$

$$\varepsilon_i = 2nK \qquad (15)$$

The values of ε_r against λ of the deposited PPFDH samples is displayed in Fig. 20 while ε_i against λ of the same sample isillustrated in Fig. 21. It is observed that both ε_r and ε_i decreases rapidly up to wavelength, 550 nm and then becomes zero which indicates the insulating nature of the films. Moreover, the plots of ε_r and ε_i against λ ensue the identical pattern and it is come into view that the values of ε_r are higher than that of the ε_i for all samples.

The dissipation factor, tan δ, can be determined by using the following relation [60]:

$$\tan \delta = \frac{\varepsilon_i}{\varepsilon_r} \qquad (16)$$

Where ε_r and ε_i is the real and imaginary part of the dielectricconstant, respectively. Fig. 22 depicts the variation of tan δ as a function of wavelength λ for all as deposited PPFDH thin films. It is found that the dissipation factor behaves anomalously with wavelength.

Optical response is most conveniently studied in terms of optical conductivity. The consequence of the variation of the optical conductivity with film thickness for as deposited PPFDH thin films were investigated to understand the optical response of the films. The optical conductivity, σ_{opt} is connected with the absorption coefficient, α, refractive index, n, and velocity of light, c by the following equation [76]:

$$\sigma_{opt} = \frac{\alpha n c}{4\pi} \qquad (17)$$

The values of optical conductivity for all as deposited PPFDH thin films were calculated using eq. (17) and plotted with varied λ as demonstrated in Fig. 23. It can be noticed that the optical conductivity reduces sharply up to wavelength 500 nm and then it become zero. The decrease of optical conductivity at higher wavelength is owing to the greater amount of absorbanceof PPFDH films at that region. In addition, it might be due to the fact that electron is excited by the energy of photon [77]. It is also observed that optical conductivity rises with rising film thickness which could be connected to the grown density of the localized states in the gap on account of the emergence of new defect states [62].

Finally, the skin depth, χ of the PPFDH films was worked out employing the relation mention below [78]:

$$\chi = \frac{\lambda}{2\pi K} \qquad (18)$$

Where K is the extinction coefficient and λ the wavelength associated with incident photon. The change of χ with photon energy, hv is presented in Fig. 24 and from this figure it is observed that χ decreases monotonically with hv for all samples.

4. Conclusions

In brief, uniform and fracture freeamorphous PPFDH thin films of 100-300 nm thicknesses were successfully prepared through glow discharge of FDH. The PPFDH samples contain asymmetric C-H and C≡C stretching bonds which form due to plasma polymerization. The obtained direct and indirect band gaps of varied thicknesses are about 3.40-3.45 and 2.10-2.45 eV, respectively and these variations of optical band gaps with thickness is owing to the improved structural shuffle in PPFDH during plasma polymerization. The value of E_u of the PPFDH thin film changes from 0.50 to 0.61 eV which may be due to some shortening of localized states in the E_q. The σ value varies from 0.042 to 0.051 with the increase in thicknesses suggesting the variation of the absorption edge with increasing thickness. The value of E_d, f, M_{-1}, M_{-3}, n_∞, ε_∞ and S_0, increases from 6.35 to 18.85

eV, 20.16 to 53.30 $(eV)^{2}$, 2.00 to 6.67 $(eV)^{-2}$, 0.20 to 0.83 $(eV)^{-2}$, 0.47 to 1.53, 0.22 to 2.34 and 1.30×10^{-5} to $3.45\times10^{-5}(nm^{-2})$ respectively. On the other hand, the value of E_0 decreases from 3.17 to 2.83 eV with increasing thickness of the PPFDH thin films. Therefore, considering all these result it may conclude that PPFDH thin films have potential uses in the devices of electronic and optoelectronic fields.

Reference

[1] H. Yasuda, Plasma polymerization, Academic Press, Orlando, (1985).

[2] C.D. Easton, M.V. Jacob, Polym. Degrad. Stab. 94 (2009) 597-603.

[3] S. Bao, Y. Yamada, M. Okada, K. Yoshimura, Appl. Surf. Sci. 253 (2007) 6268-6272.

[4] H. Biederman and Y. Osada, Plasma Chemistry of Polymers, Advance in Polym. Sci., Berlin (1990).

[5] L. J. Anderson, M. V. Jacob, Appl. Surf. Sci. 256 (2010) 3293-3298.

[6] X. Y. Zhao, M. Z. Wang and J. Xiao, Euro. Polym J., 42(2006) 2161-2167.

[7] J. Ahmad, K. Bazaka and M. V. Jacob, Electronics 3 (2014) 266-281.

[8] G. B.V. S. Lakshmi, A. Dhilon, A. M. Siddique, M. Zulfequar, D. K. Avasthi, Euro. Polym J., 45 (2009) 2873-2877.

[9] C. J. Mathai, S. Saravanan, M. R. Anantharaman, S. Venkitachalam and S. Jayalekshmi, J. Phys. D Appl. Phys., 35 (2002) 240-245.

[10] H. Yasuda, Luminous Chemical Vapor Deposition and Interface Engineering, CRC, New York, (2004).

[11] K. Bazaka, M. V. Jacob, W. Chrzanowski and K. Ostrikov, RSC Advance 5, (2015) 48739-48759.

[12] I. -S. Bae, S. -H. Cho, S. -B. Lee, Y. Kim, J. -H. Boo, Surf. & Coat. Technol., 193 (2005) 142-146.

[13] D. S. Kumar, M. Fujioka, K. Asano, A. Shoji, A. Jayakrishnan, Y. Yoshida, J. Mater. Sci., Mater Med., 18 (2007) 1831–1835.

[14] H. Biederman and Y. Osada, Plasma Polymerization Processes, Elsevier: Amsterdam, (1992).

[15] M. V. Jacob, C. D. Easton, G. S. Woods, C. C. Berndt, Thin Solid Films 516 (2008) 3884-3887.

[16] D. Hegemann, M. M. Hossain, E. Korner and D. J. Balazs, Plasma Process. Polym.,4 (2007) 229-238.

[17] K. Bazaka and M. V. Jacob, Materials Letters 63 (2009) 1594-1597.

[18] M. M. El-Nahass, H. M. Zeyada, M. M. El-Samanoudy, E. M. El-Menyawy, J. Phys. Condens. Matter. 18 (2006) 5163-5170.

[19] T.C.M. Santhosh, Kasturi V. Bangera, G.K. Shivakumar, J. Alloys Compd. 703 (2017) 40-44.

[20] R Jayasekara, ,I Harding, I Bowater, G.B.Y Christie, G.T Lonergan, Polym. Testing 23 (2004) 17-27.

[21] G. Riveros, C. Baez, D. Ramírez, C. J. Pereyra, R. E. Marotti, R. Romero, F. Martín, J. R. Ramos-Barrado, E. A. Dalchiele, J. Alloys Compd. 686 (2016) 235-244.

[22] M. V. Jacob, N. S. Olsen, L. J. Anderson, K. Bazaka, R. A. Shanks, Thin Solid Films 546 (2013) 167-170.

[23] F.-U.-Z. Chowdhury and A.H. Bhuiyan, Thin Solid Films 360 (2000) 69-74.

[24] J. Moosburger-Will, M. Bauer, F. Schubert, C. Kunzmann, E. Lachner, H. Zeininger, M. Maleika, B. Hönisch, J. Küpfer, N. Zschoerper, Surf. & Coat. Technol., 311(2017) 223–230.

[25] A. Amri, Z.- T. Jiang, C.- Y. Yin, A. Fadli, M. M. Rahman, S. Bahri, H. Widjaja, N. Mondinos, T. Herawan, M. M. Munir, G. Priyotomo, Physica status solidi 213 (2016) 3205-3213.

[26] A. Amri, X. F. Duan, C. Y. Yin, Z. T. Jiang, M. M. Rahman and T. Pryor, Appl. Surf. Scien. 275 (2013) 127-135.

[27] J. López, E. Solorio, H. A. Borbón-Nuñez, F. F. Castillón, R. Machorro, N. Nedev, M. H. Farías, H. Tiznado, J. Alloys Compd. 691 (2017) 308-315.

[28] M. M. Rahman, Z.-T. Jiang, P. Munroe, L. S. Chuah, Z. –f. Zhou, Z. Xie, C. Y. Yin, K. Ibrahim, A. Amri, H. Kabir, M. M. Haque, N. Mondinos, M. Altarawneh and B. Z. Dlugogorski, RSC Advances, 6 (2016) 36373-36383.

[29] H. J. Shin, S. Kang, J. Y. Baik, I. Lee, P. Singh, A. Thakur, J. Phys. Chem. Solids, 80(2015) 7–10.

[30] Z.B. Zhou, R.Q. Cui, Q.J. Pang, G.M. Hadi, Z.M. Ding, W.Y. Li, Sol. Energy Mater. Sol. Cells 70 (2002) 487.

[31] D. Rossi, W. H. Schreiner, S. F. Durrant, Surf. & Coat. Technol., 289 (2016) 118–123.

[32] A. Mukherjee, M. Fu, P. Mitra, J. Phys. Chem. Solids, 82 (2015) 50-55.

[33] L. Martin, J. Esteve and S. Borros, Thin Solid Films 452 **(**2004) 74-80.

[34] N. Inagaki and Y. Tano, J. PolymSci, Polym Chem. 25 (1987) 1197-1203.

[35] N. Jahan, R. Matin, M. S. Bashar, M. Sultana, M. Rahaman , M. A. Gafur, M. A. Hakim, H. Kabir, M. K. Hossain, F. Ahmed, American Int. J. Res. Sci. Techno., Eng. &Mathem. 1 (2016) 69-73.

[36] R. Anuroop, B. Pradeep, J. Alloys Compd. 702 (2017) 432-441.

[37] H. Kabir, M. M. Rahman, T. S. Roy and A. H. Bhuiyan, Int. J. Mech. Mechatron. Eng.12 (2012) 30-34.

[38] G.Ke, Y. Tao, Z. He, H.Guo, Y. Chen, J.DiBattista, E.Chan,Y. Yang, Surf. & Coat. Technol., 289 (2016) 87–93.

[39] A. Bradley and J. P. Hammes, J. Electrochem Soc. 110 (1963) 15-22.

[40] F. -U. -Z. Chowdhury, A. B. M. O. Islam, A. H. Bhuiyan, Vacuum 57 (2000) 43-50.

[41] S. Islam, M. A. Hossain, H. Kabir, M. Rahaman, M. S. Bashar, M. A. Gafur, A. Kabir, M. M. R. Bhuiyan, F. Ahmed, N. Khatun, Int. J. Thin Films Sci. Techno. 4 (2015) 155-161.

[42] R. Matin and A. H. Bhuiyan, Thin Solid Films 534 (2013) 100-106.

[43] I. Blaszczyk-Lezak, F. J. Aparicio, A. Borra´s, A. Barranco, A. Alvarez-Herrero, M. Ferna´ndez-Rodrı´guez and A. R. Gonza´lez-Elipe, J. Phys. Chem. C, 113 (2009)431-438.

[44] S.-J. Cho, I.-S. Bae, J.-H. Boo, Y. S. Park, and B. Hong, J. Korean Phys. Soc., 53 (2008) 1634-1637.

[45] T. Afroze and A. H. Bhuiyan, Thin Solid Films 519 (2011) 1825-1830.

[46] M. M. Kamal, and A. H. Bhuiyan, J. Appl. Polymer Science 121 (2011) 2361-2368.

[47] R. B. Sarker and A. H. Bhuiyan, Int. J. Moder. Phys. B 25 (2011) 1941-1955.

[48] S. Majumder and A. H. Bhuiyan,Advan. Polym. Techno. 34 (2014) 21468.

[49] R. Matin and A. H.Bhuiyan, J. Phys. Chem. of Solids, 75(2014) 1179-1186.

[50] H. Kabir, A. H. Bhuiyan, M. M. Rahman, Thin Solid Films 609 (2016) 35-41.

[51] S. Tolansky, Multiple beam Interferometry of Surfaces and Films, ClarendonPress, Oxford, 1948.

[52] Frisch, M.; Trucks, G.; Schlegel, H. B.; Scuseria, G.; Robb, M.; Cheeseman, J.; Scalmani, G.; Barone, V.; Mennucci, B.; Petersson, G., Gaussian 09, Revision A. 02, Gaussian. *Inc., Wallingford, CT* **2009**, 200.

[53] O. D. Coskun and S. Demirel, Appl. Surf. Sci. 277 (2013) 35-39.

[54] M. J. Rahman, A.H. Bhuiyan, Thin Solid Films 534 (2013) 132-136.

[55] D. E. Milovzorov, A. M. Ali, T. Inkuma, Y. Kurata, T. Suzuki, S. Hasegawa, Thin Solid Films 382 (2001) 47-55.

[56] S. Kalyanaraman, P.M. Shajinshinu, S.Vijayalakshmi, J.Phys.Chem. Solids **86** (2015) 108–113.

[57] J. Tauc, A. Menth, D. Wood, Phys. Rev. Lett., **25**, (1970)749-752.

[58] S. Ilican, M. Caglar, Y. Caglar, Mat. Sci.Poland 25(2007) 709-718.

[59] M. S. Hossain, H.Kabir, M. M.Rahmana, K. Hasan, M. S. Bashar, M. Rahman, M. A.Gafur, S. Islam, A.Amri, Z.T. Jiang, M.Altarawneh, B. Z. Dlugogorski, Appl. Surf. Sci. 392 (2017) 854–862.

[60] F. Urbach, Rev. **92**, (1953) 1324-1330.

[61] S. A.Fayek,M. R.Balboul, K. H.Marzouk, Thin Solid Films **515** (2007) 7281-7286.

[62] H.Mahr, Phys. Rev.**125**(1962) 1510-1515.

[63] M.M. Abdel-Aziz, I.S. Yahia, L.A. Wahab, M. Fadel, M.A. Afifi, Appl. Surf. Sci. **252** (2006) 8163–8170.

[64] M. Didomenico, S.H. Wemple, J. Appl. Phys. 40 (1969) 720-725.

[65] S. H.Wemple, Didomenico, Phys. Rev., B3 (1971) 1338-1351.

[66] S. H. Wemple, Phys. Rev., B7, (1973) 3767-3777.

[67] I. C. Ndukwe Sol. Ener. Mater. and Sol. Cells 40**(1996)**123-130.

[68] D.J. Gravesteijn, Appl. Opt. 27 (1988) 736-740.

[69] S. H. Wemple, M. DiDomenico, Phys. Rev. Lett. 23 (1969) 1156-1162.

[70] S. H.Wemple, DiDomenico, J. Appl. Phys. 40 (1969) 720-734.

[71] F. Yakuphanoglu, A. Cukurovali, I. Yilmaz, Physica B 351 (2004) 53-60.

[72] M. El-Hagary, M. Emam-Ismail,, E.R. Shaaban, A. Al-Rashidi, S. Althoyaib, Mat. Chem. Phys. 132 (2012) 581– 590.

[73] S.H. Wemple, DiDomenico, Phys. Rev. B 3 (1971) 1338.

[74] A. El-Korashy, H. El-Zahed, M. Radwan, Physica B 334 (2003) 75-80.

[75] M.M. Wakad, E.Kh. Shokr, S.H. Mohammed, J. Non-Cryst. Solids 265(2000) 157.

[76] J.I. Pankove, Optical Processes in Semiconductors, Dover Publications Inc., New York, 1975.

[77] F. Yakuphanoglu, A. Cukurovali, I. Yilmaz, Opt. Mater. 27 (2005) 1366.

[78] J. F. Eloy, Power Lasers, National School of Physics, Grenoble, France, John Wiley and Sons, 59, 1984.

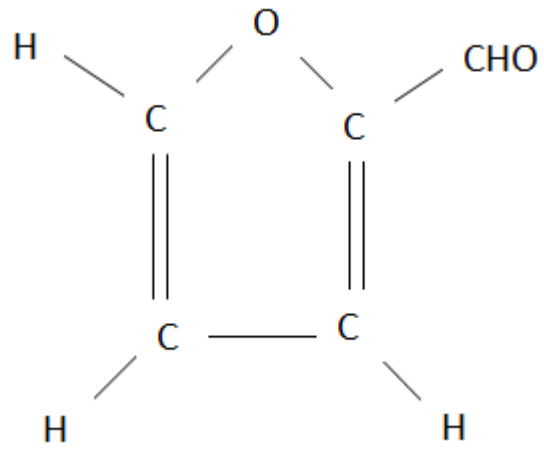

Fig.1.The chemical structureof 2-furaldehyde

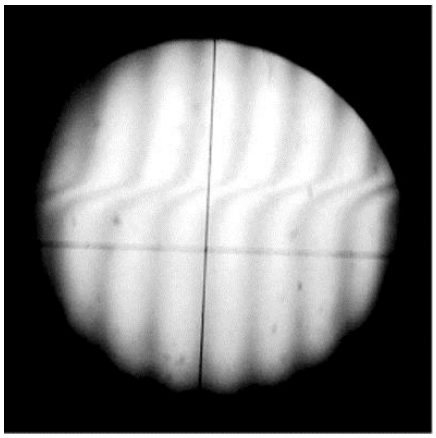

Fig. 2. The Fizeau fringe pattern of PPFDH thin film.

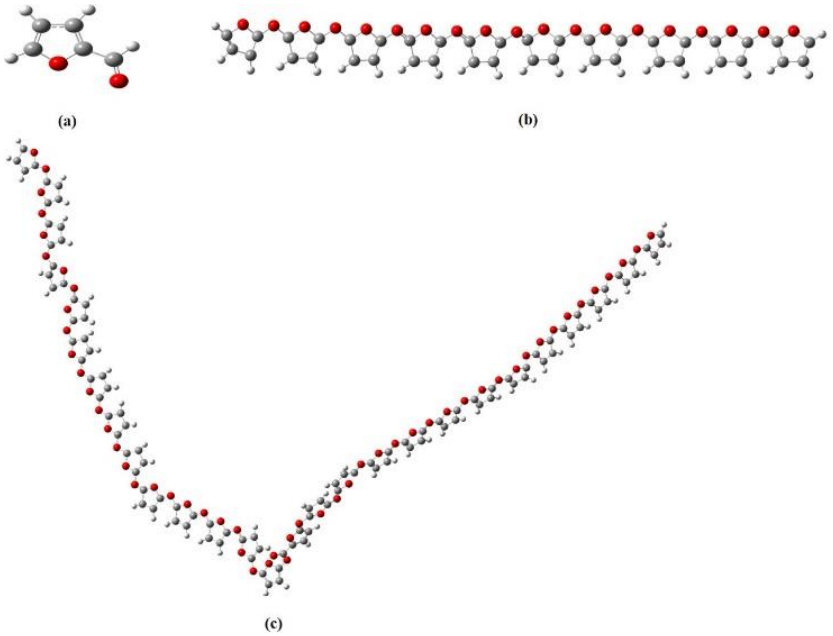

Fig. 3. Optimized structures of monomer (a) and polymers (b and c) for2-furaldehyde.

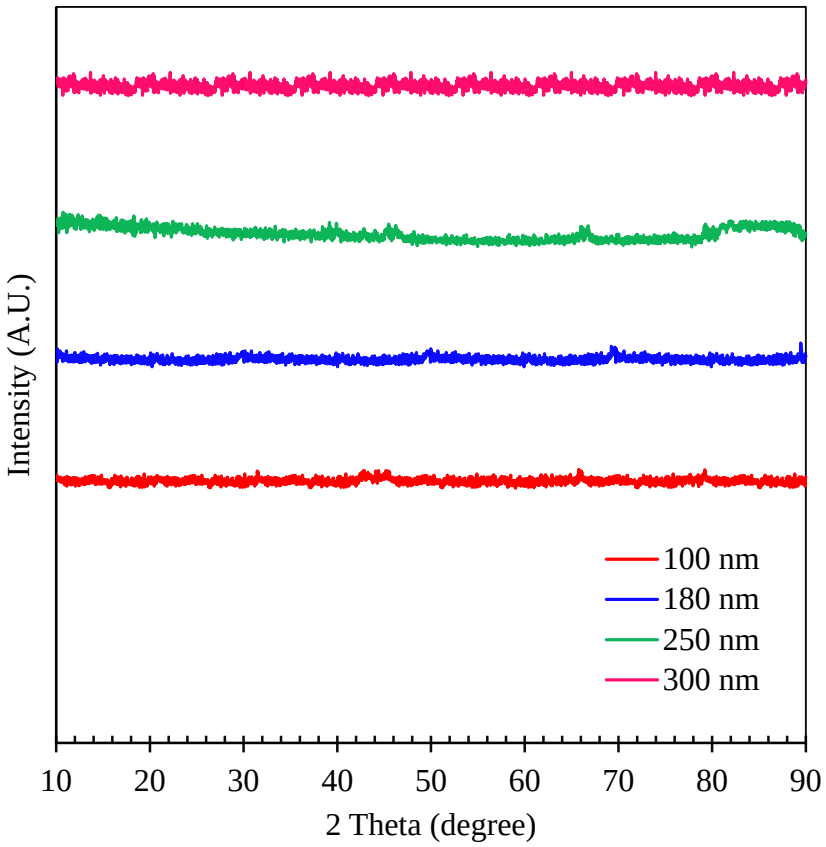

Fig.4. X-Ray diffraction patterns of as deposited PPFDH thin films at different thicknesses

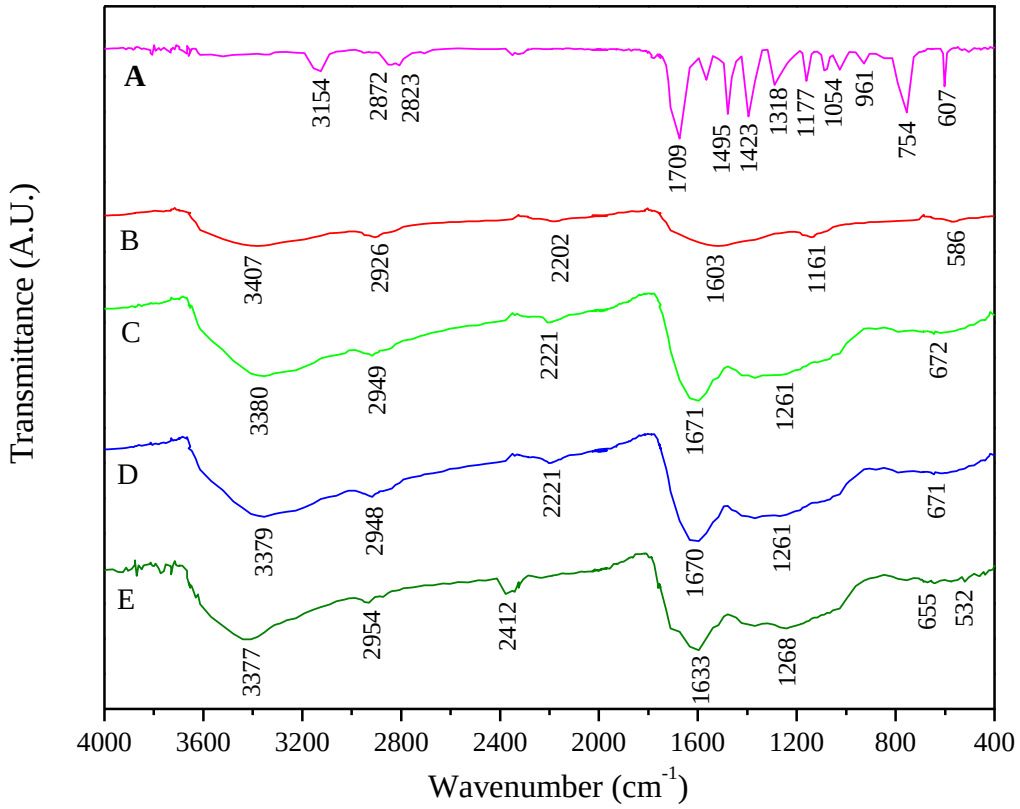

Fig. 5. The FTIR spectra for FDH (A) and PPFDH at different thicknesses, (B) t=100 nm, (C) t=180 nm, (D) t=250 nm and (E) t=300 nm.

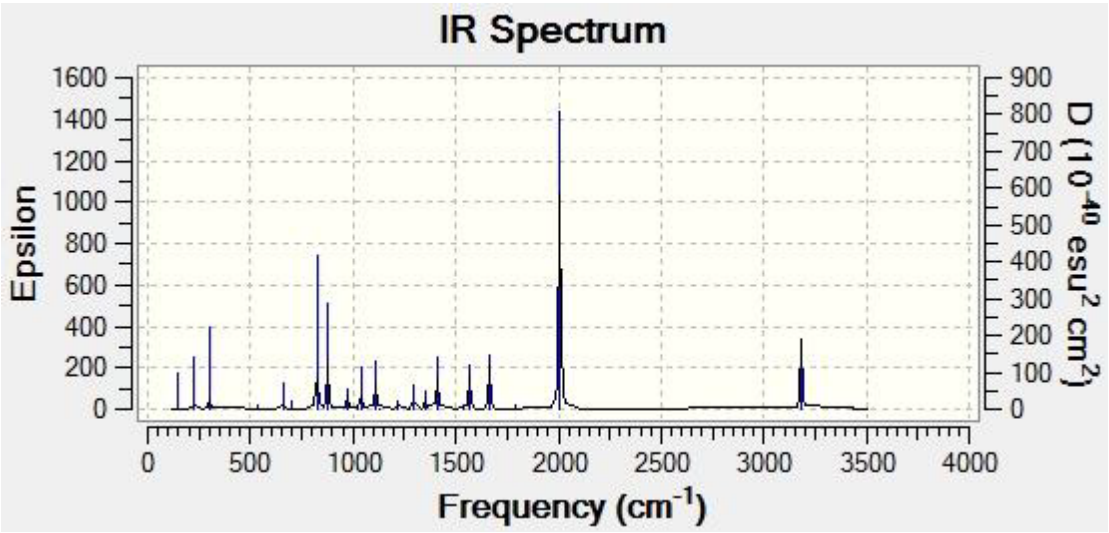

Fig. 6. Theoretical IR spectrum of 2-furaldehyde

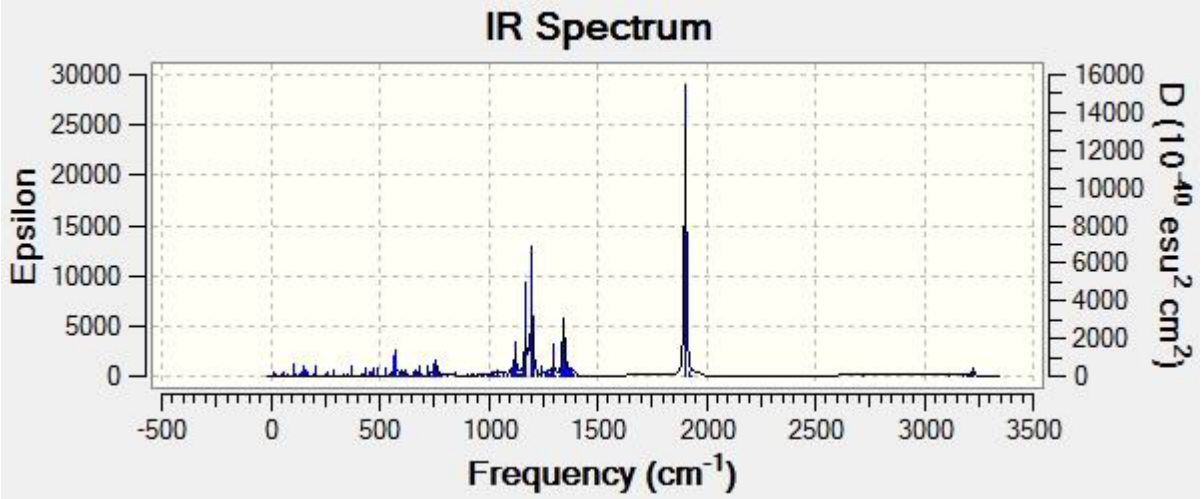

Fig. 7. Theoretical IR spectrum of polymer for 2-furaldehyde.

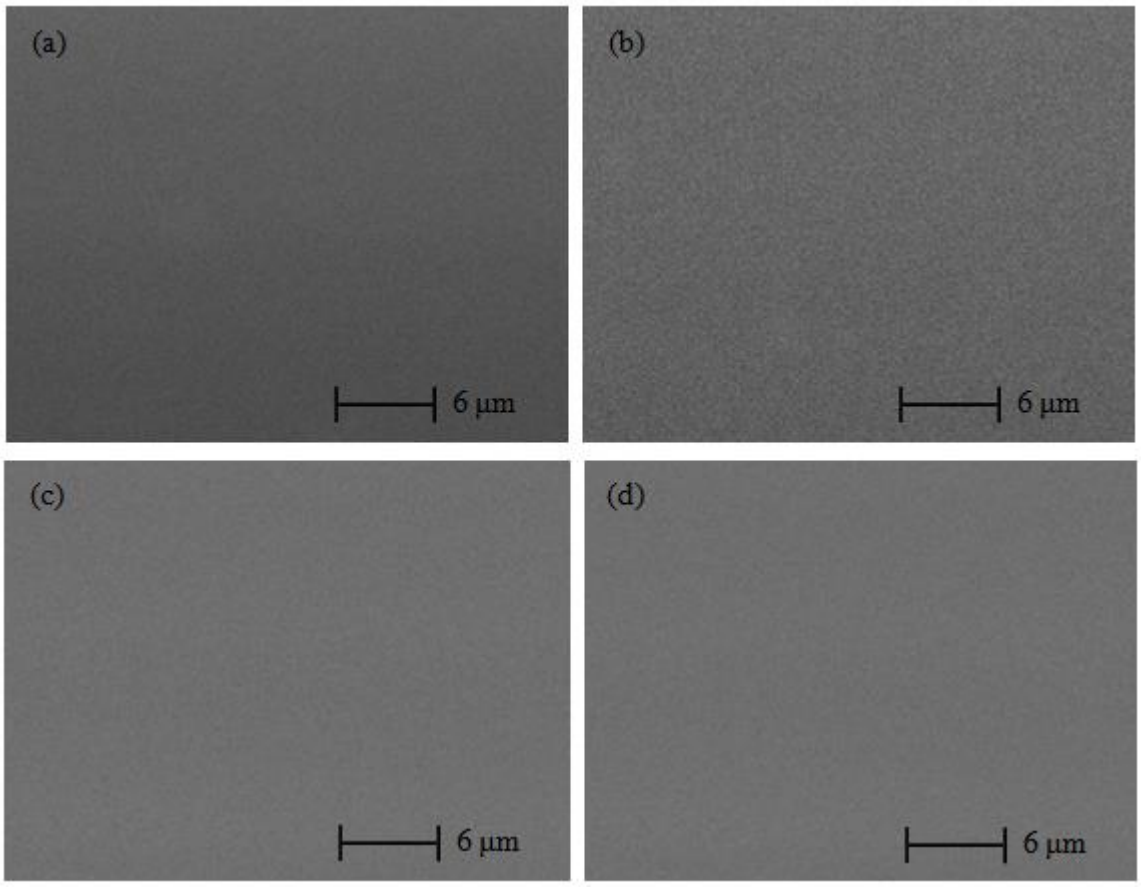

Fig. 8. SEM micrographs of the PPFDH thin films of different thicknesses at 25k×, (a) t=100 nm, (b) t=180 nm, (c) t=250 nm and (d) t=300 nm.

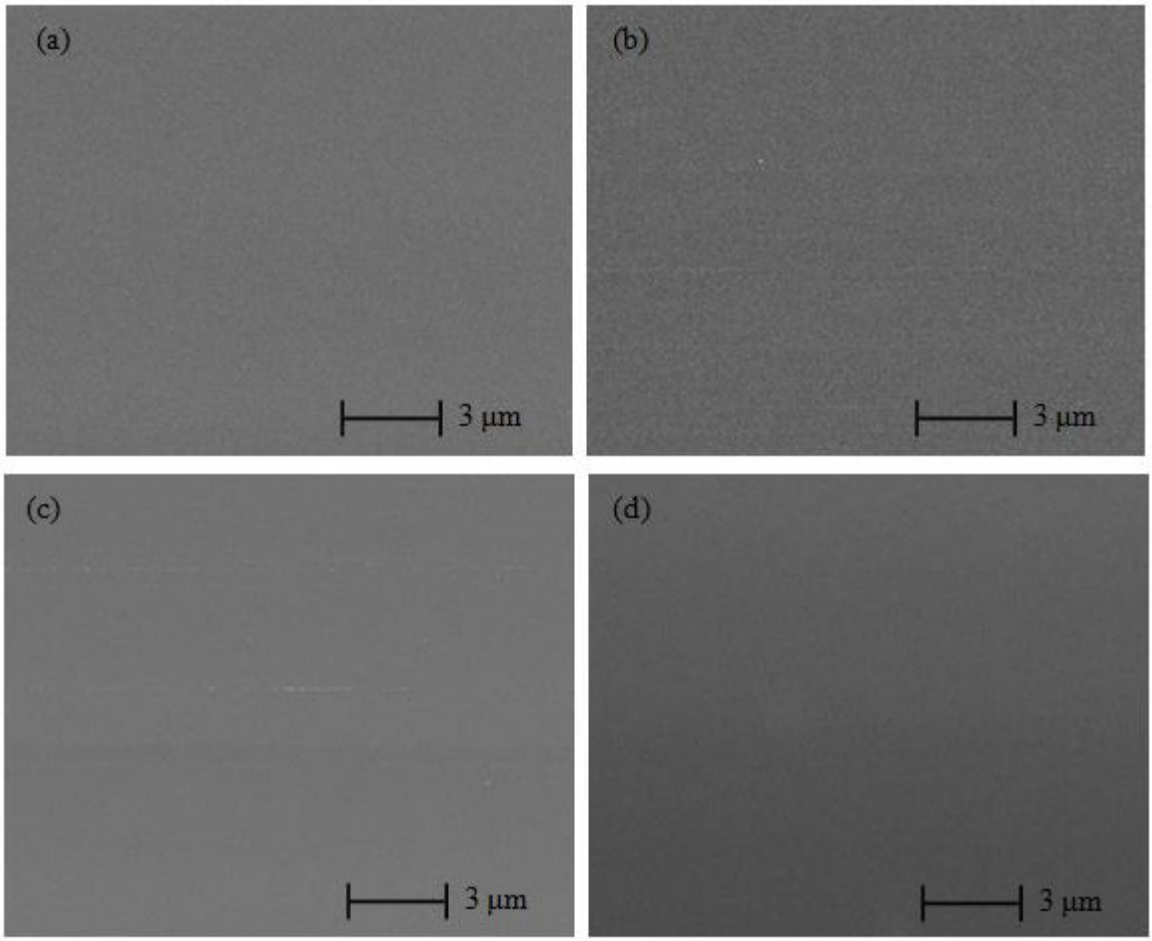

Fig. 9.SEM micrographs of the PPFDH thin films of different thicknesses at 50k×, (a) t=100 nm, (b) t=180 nm, (c) t=250 nm and (d) t=300 nm.

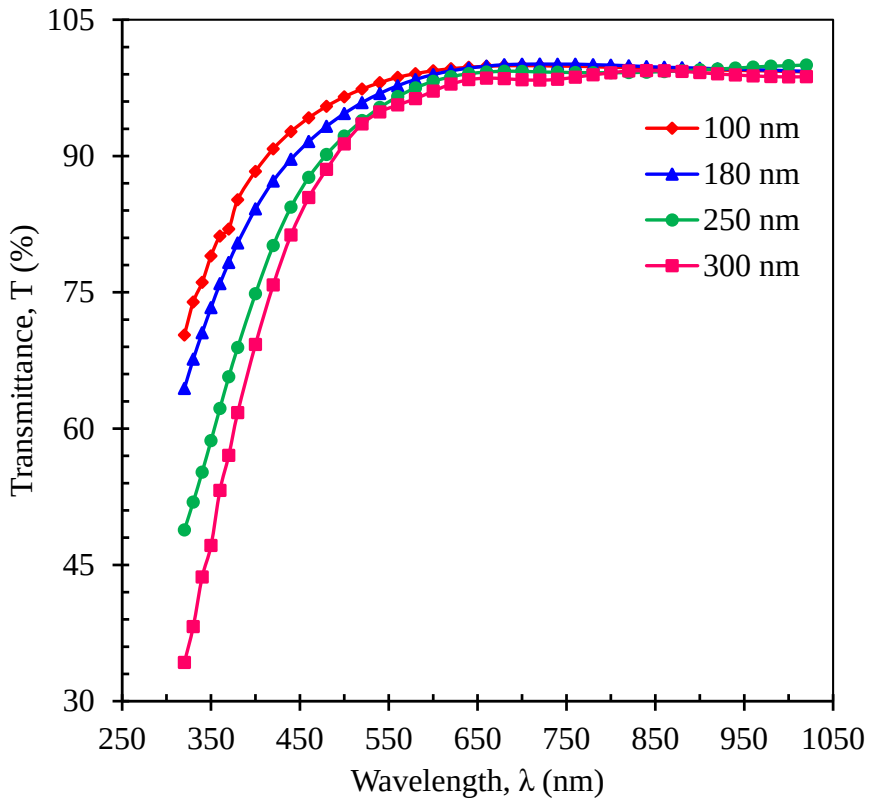

Fig. 10. Spectral distribution of transmittance $T(\lambda)$ at different thicknesses.

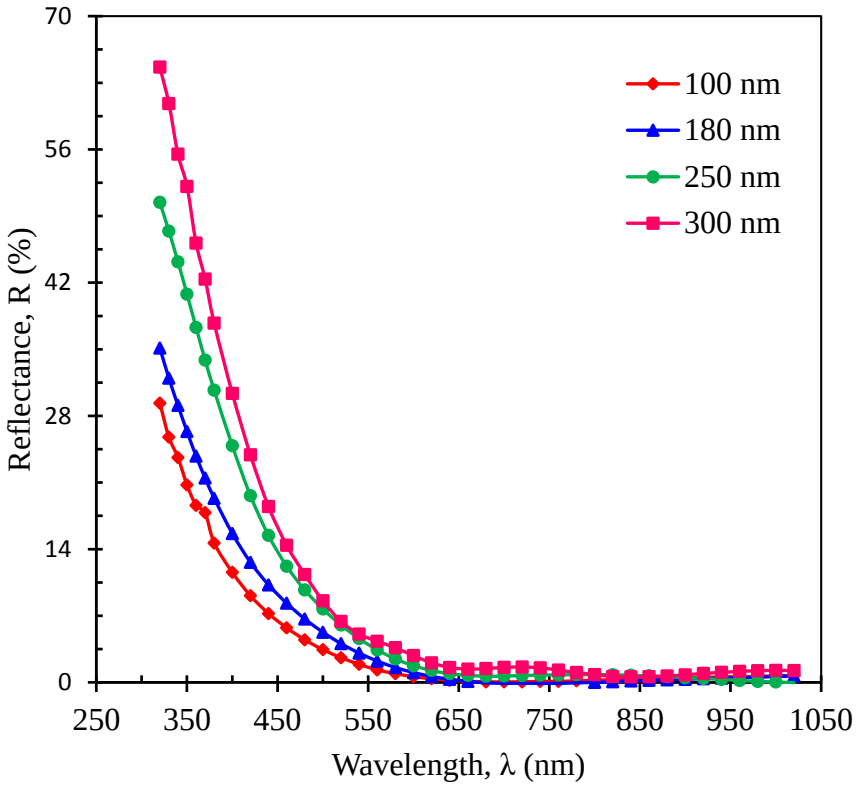

Fig. 11.Spectral distribution of reflectance $R(\lambda)$ at different thicknesses.

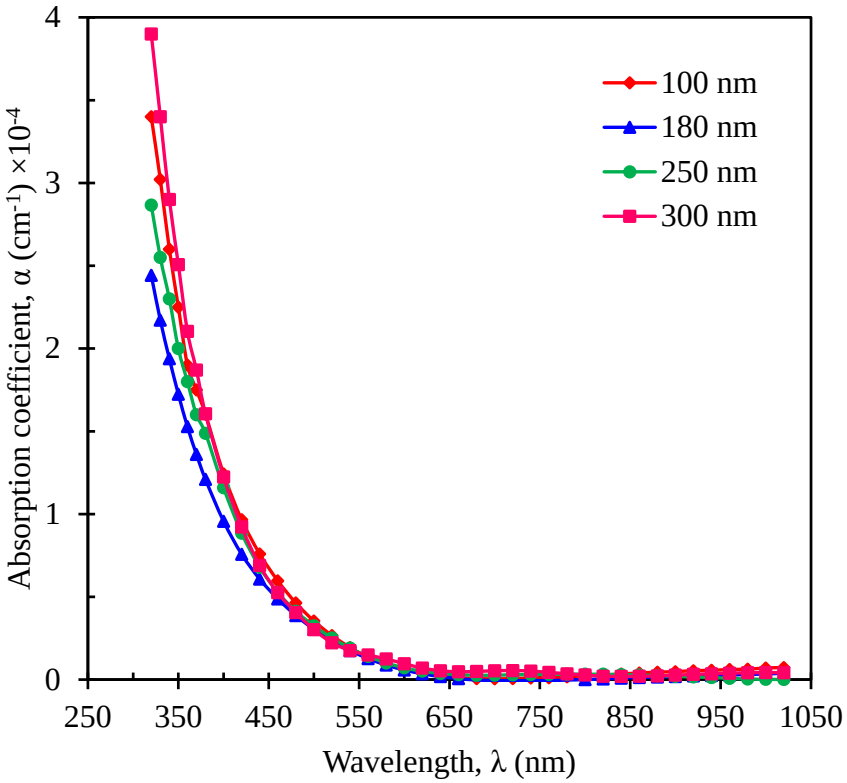

Fig. 12. Plot of α with $h\nu$, for as-deposited PPFDH thin films of different thicknesses.

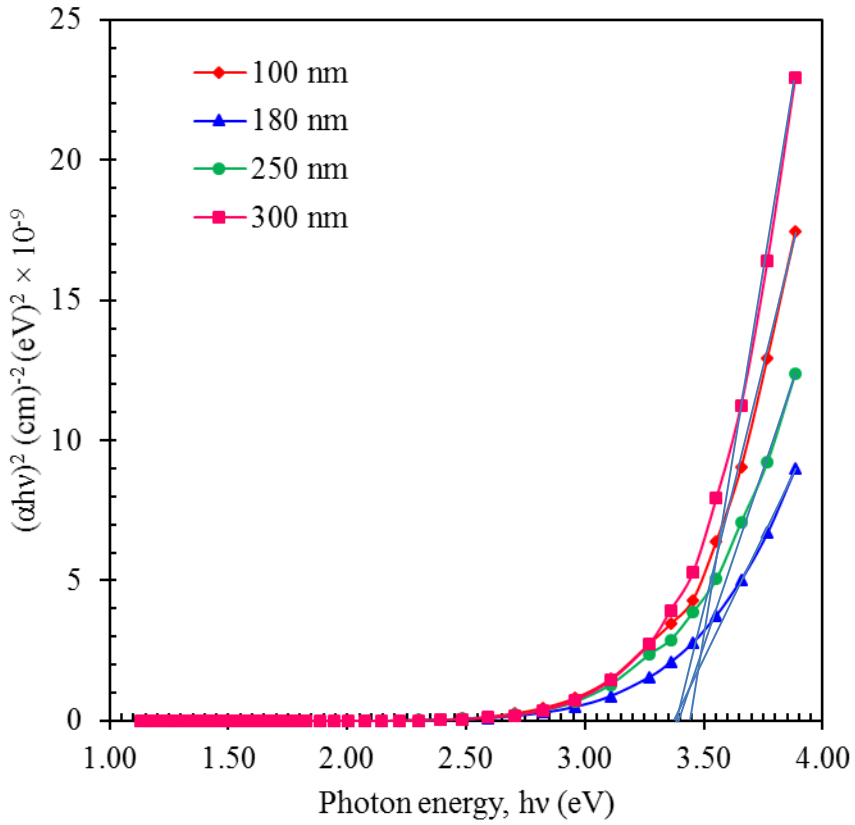

Fig. 13. The plot of $(\alpha h\nu)^2$ vs $h\nu$, for all as-deposited PPFDH thin films.

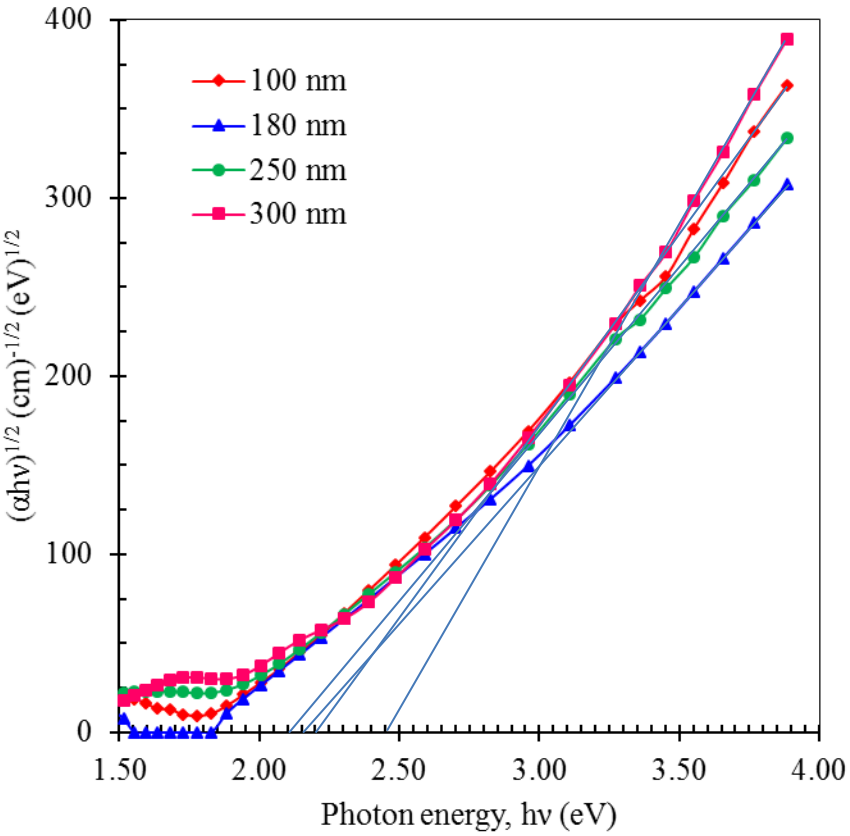

Fig. 14. The plot of $(\alpha h\nu)^{1/2}$ vs $h\nu$, for all as-deposited PPFDH thin films.

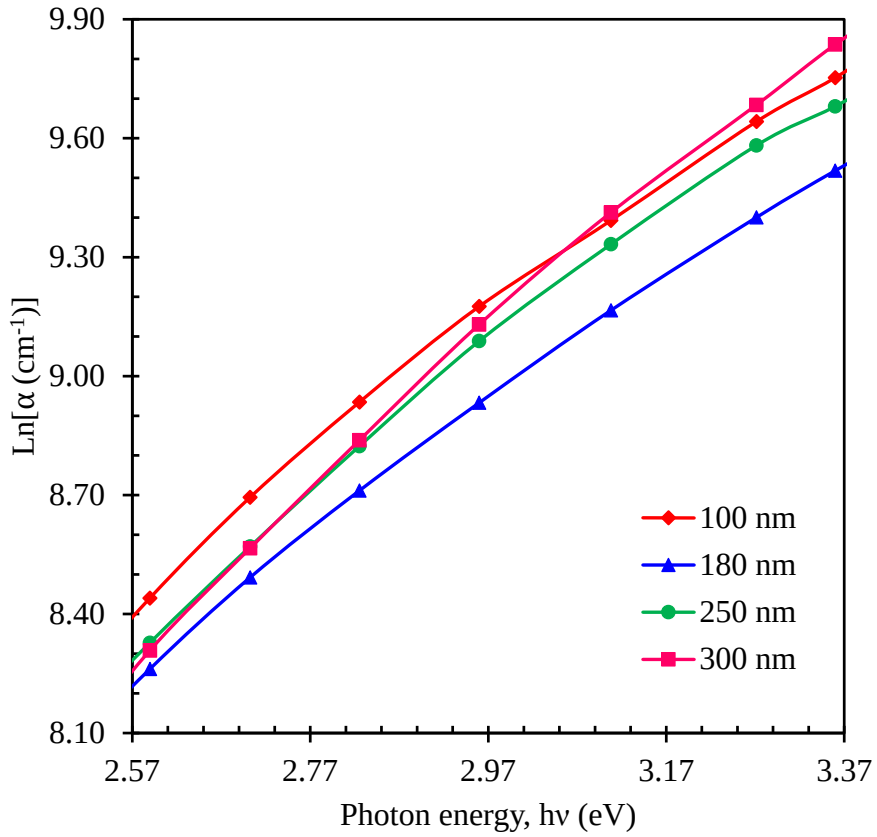

Fig. 15. The Ln*α* vs *hν* plots for all as deposited PPFDH thin films.

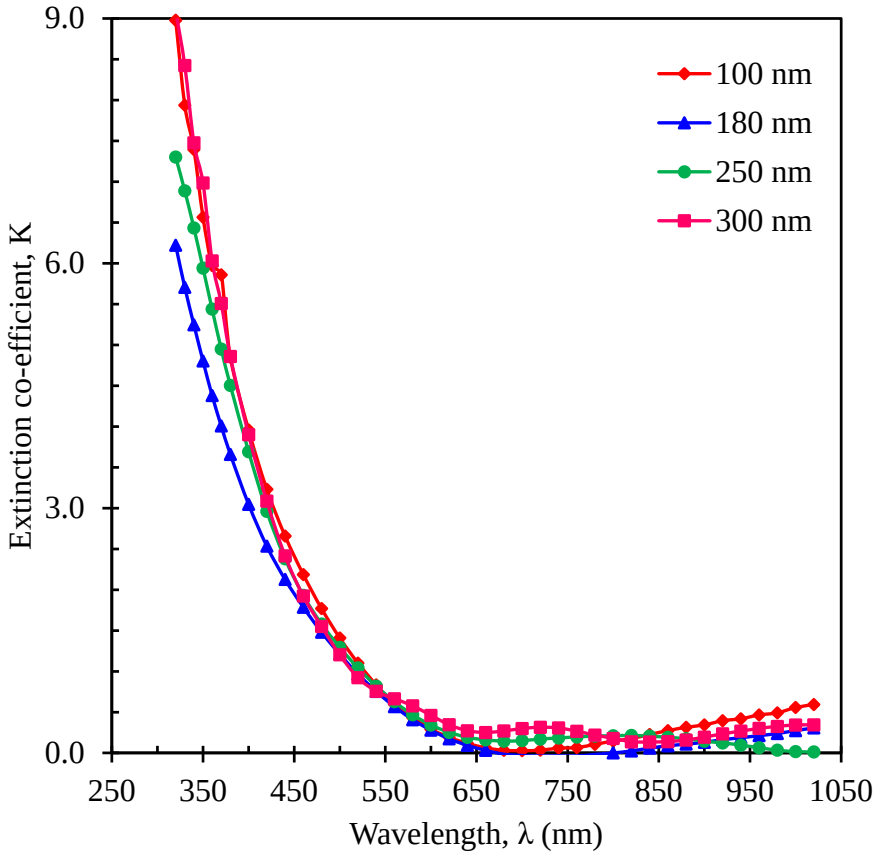

Fig. 16.The variation of *K* for all as deposited PPFDH thin films with λ.

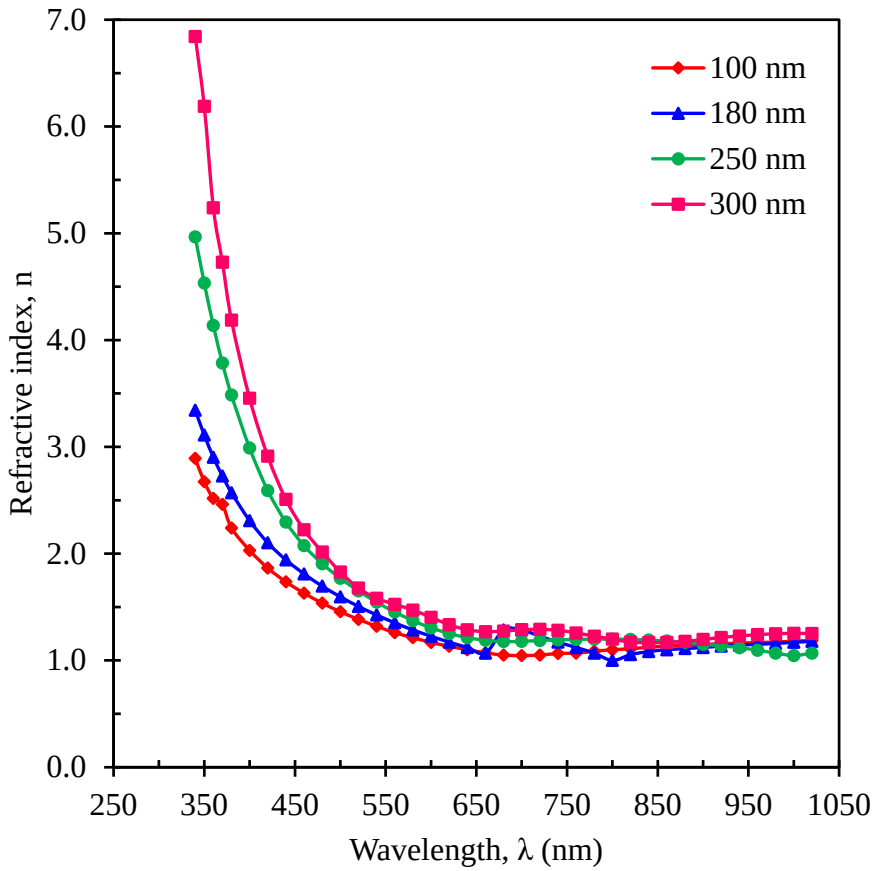

Fig. 17.The change in *n* for all as deposited PPFDH thin films with *λ*.

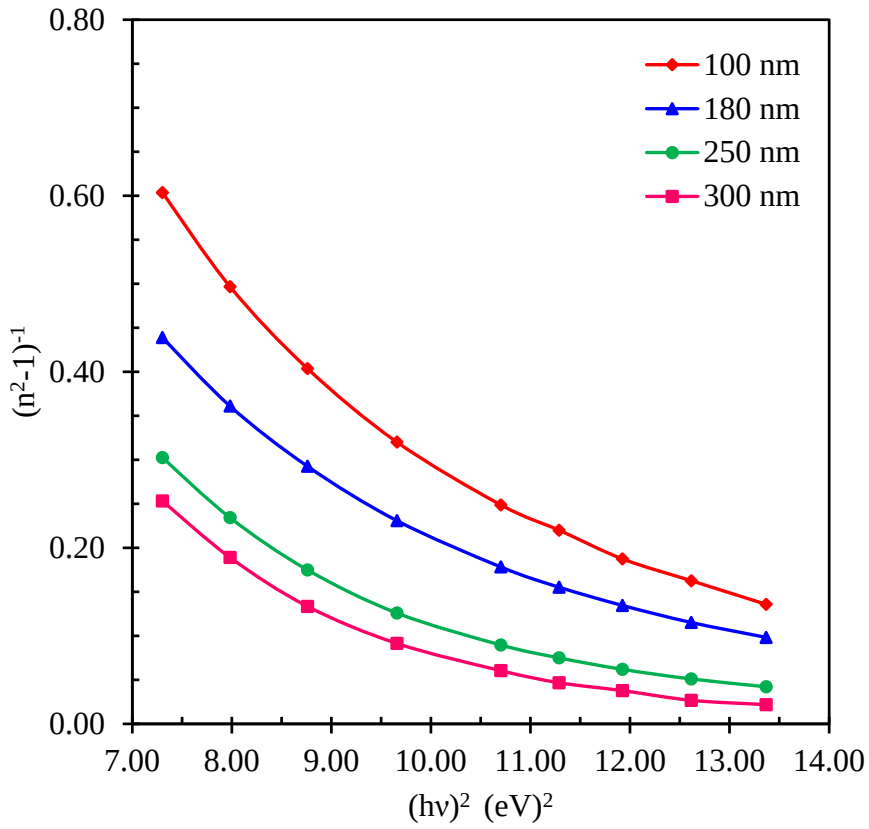

Fig.18. Plot of $(n^2-1)^{-1}$ versus $(hv)^2$ of all as deposited PPFDHthin films.

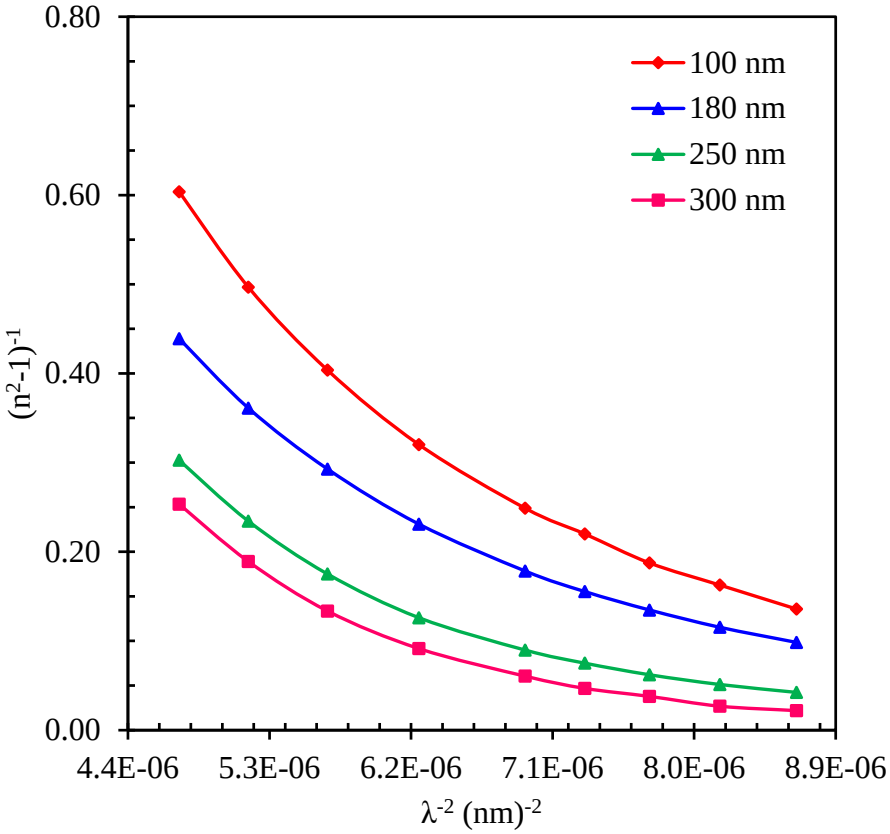

Fig.19. Plot of $(n^2-1)^{-1}$ versus λ^{-2} of all as deposited PPFDH thin films.

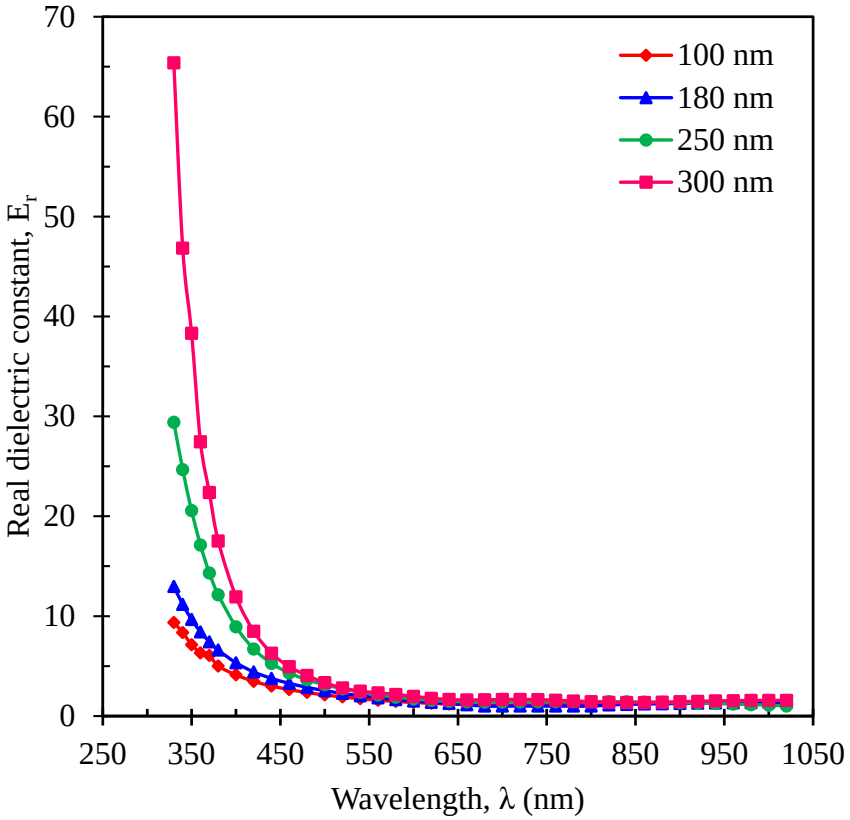

Fig.20. Plot of ε_r as a function of λ for all as deposited PPFDH thin films.

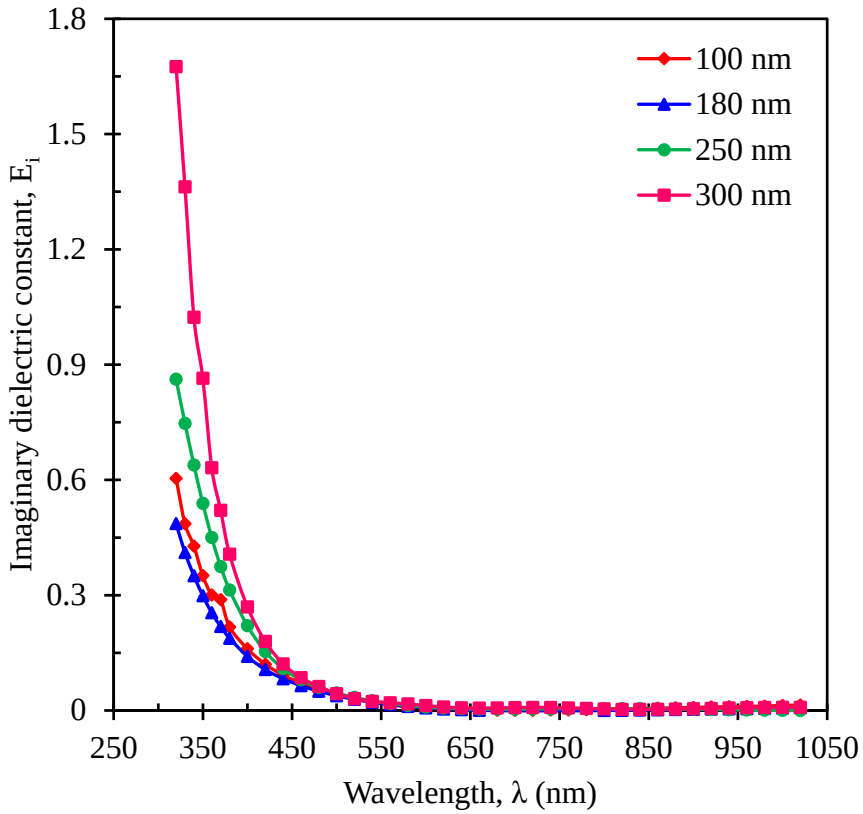

Fig.21. Plot of ε_i as a function of λ for all as deposited PPFDH thin films.

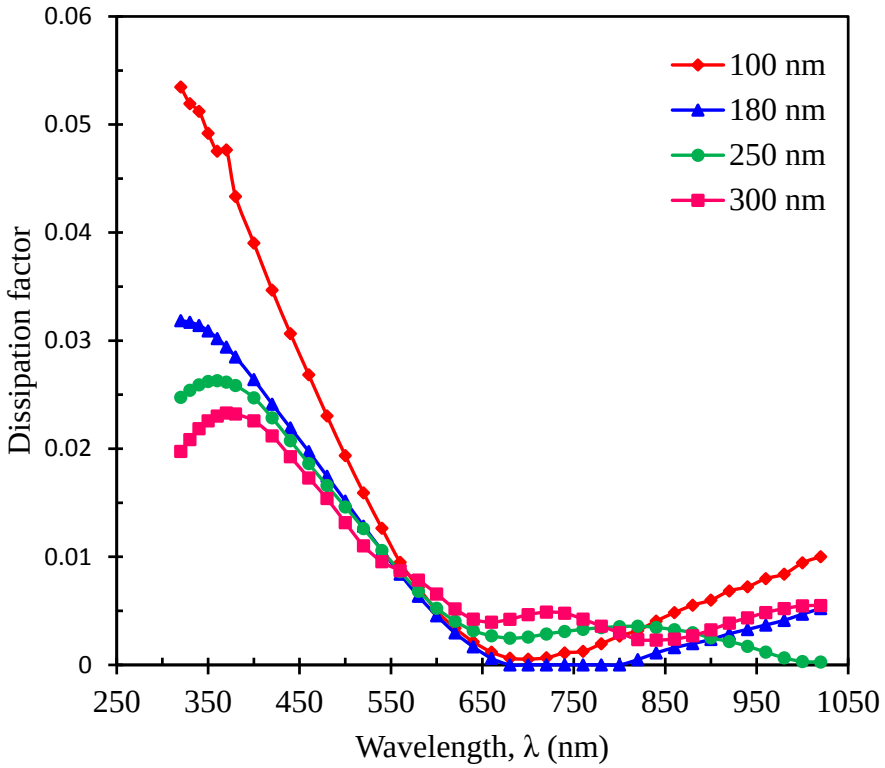

Fig.22. Plot of tan δ as a function of λ for all as deposited PPFDH thin films.

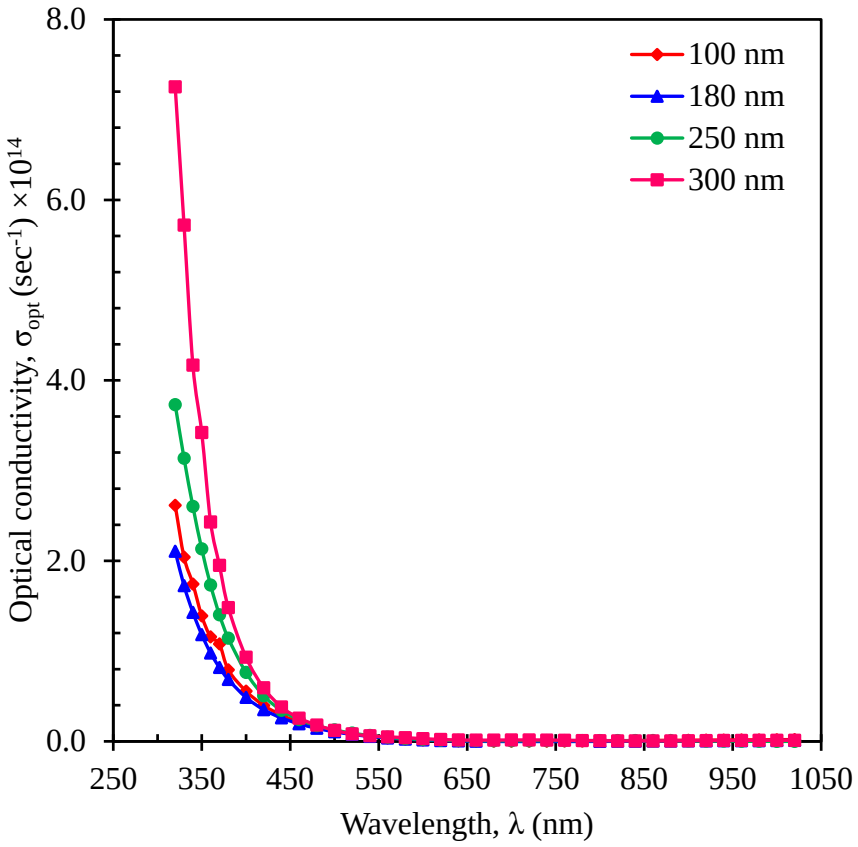

Fig. 23. The variation of σ_{opt} for all as deposited PPFDH thin films with λ.

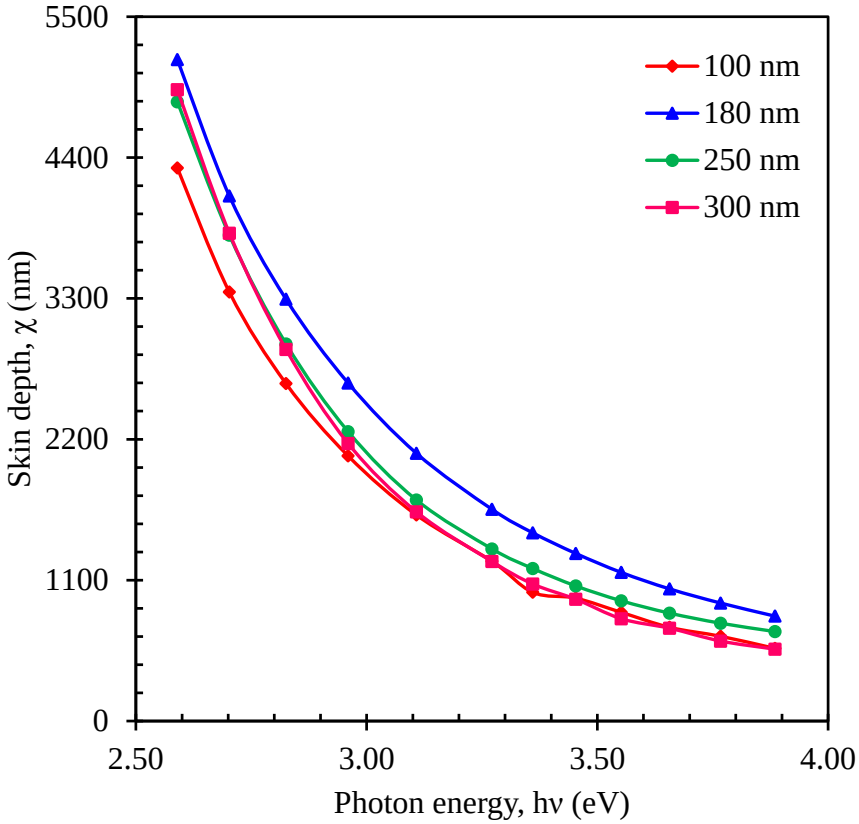

Fig. 24. The change in χ for all as deposited PPFDH thin films with *hv*.

Table 1 General properties of 2-furaldehyde

Commercial Name	Furfural
IUPAC name	2-furaldehyde
Form	Clear liquid
Colour	Colourless oil
Molecular formula	$C_5H_4O_2$
Chemical formula	OC_4H_3CHO
Molecular weight	96.0841 g/mol
Density	1.160 g/cm^3
Freezing point	-37 °C
Boiling point	162 °C
Flash point	62 °C

Table 2 Assignments of FTIR absorption peaks for FDH and PPFDH of different Thicknesses

Assignments	Wavenumber (cm^{-1})						
	Monomer		As deposited PPFDH				
	FDH (A)	Calc.	B	C	D	E	Calc.
O-H stretching	3154	3183	3407	3380	3379	3377	3325
Asym. C-H	-------	-------	2926	2949	2948	2954	2971
Aliphatic -O-CH_3	2872,	2913	-------	-------	-------	-------	-------
C≡C stretching	-------	-------	2202	2221	2221	2412	2213
C=C stretching	1709	1664	1603	1671	1670	1633	1662
Asym.C-H	1495,1423	1535,	-------	-------	-------	-------	-------
Symmetric C-H	1318	1303	-------	-------	-------	-------	-------
C-H twisting	1277	1256	1161	1261	1261	1268	1260
C-C skeletal	1177	1213	-------	-------	-------	-------	-------
C=H plane	1054	1038	-------	-------	-------	-------	-------
C-H rocking	961	971	-------	-------	-------	-------	-------
=C-H out of plane	754	766	-------	-------	-------	-------	-------
C=C out-of-plane	607	609	586	672	671	655,	663

Table 3 Elements detected by EDS in as-deposited PPFDH thin films

Elements detected (wt.%)	FDH (Calculated from molecular formula)	As deposited PPFDH films at different thicknesses			
		100 nm	180 nm	250 nm	300 nm
C	62.50	46.41	46.95	47.45	97.05
O	33.30	23.10	23.20	24.80	25.15
H	4.20	-------	-------	-------	-------
Na	----------	4.22	4.18	4.18	3.08
Mg	----------	1.68	1.69	1.64	1.64
Si	----------	18.78	18.18	17.08	16.73
Ca	----------	5.81	5.80	4.85	4.35

Table 4 Variations of optical parameters for as deposited PPFDH thin films at different thicknesses.

Thickness, $t \pm 5$ (nm)	Direct band gap, E_{dg} (eV) ± 0.01	Indirect band gap, E_{ig} (eV) ±0.01	Band edge sharpness, P_s ($cm^{-2}eV^{-1}$) ±0.02	Urbach energy, E_u (eV) ± 0.01	Steepness parameter, $\sigma \pm 0.001$
100	3.40	2.20	3.32×10^{-8}	0.59	0.044
180	3.41	2.15	1.58×10^{-8}	0.61	0.042
250	3.42	2.10	2.20×10^{-8}	0.56	0.046
300	3.45	2.45	4.50×10^{-8}	0.50	0.051

Table 5 Change of dispersion parameters for as deposited PPFDH thin films at different thicknesses.

Thickness, $t \pm 5$ (nm)	Dispersion energy, E_d (eV) ± 0.01	Oscillator energy, E_0 (eV) ± 0.01	Oscillator strength, f $(eV)^2 \pm 0.01$	Moments of optical spectra $(eV)^{-2} \pm 0.01$	
				M_{-1}	M_{-3}
100	6.35	3.17	20.16	2.00	0.20
180	8.94	3.13	27.97	2.85	0.29
250	14.18	3.12	44.23	4.54	0.46
300	18.85	2.83	53.30	6.67	0.83

Table 6 Values of n_∞, ε_∞, λ_∞ and S_0 for as deposited PPFDH thin films at different thicknesses.

Thickness, $t \pm 5$ (nm)	Refractive index, n_∞ ± 0.01	Dielectric constant, ε_∞ ± 0.01	Wavelength, λ_∞ (nm) ± 0.01	Average oscilator strength, S_0 (nm^{-2}) ± 0.01
100	0.47	0.22	438.12	1.30×10^{-5}
180	0.69	0.48	429.10	1.81×10^{-5}
250	1.36	1.85	482.42	2.84×10^{-5}
300	1.53	2.34	538.46	3.45×10^{-5}